Available online at www.sciencedirect.com
SCIENCE DIRECT®
Journal of Sound and Vibration 267 (2003) 209–225
JOURNAL OF SOUND AND VIBRATION
www.elsevier.com/locate/jsvi

Dynamic stability of a rotating beam with a constrained damping layer

Chung-Yi Lin*, Lien-Wen Chen

Department of Mechanical Engineering, National Cheng Kung University, Tainan 70101, Taiwan, ROC

Received 21 February 2002; accepted 14 October 2002

Abstract

The dynamic behavior and dynamic instability of the rotating sandwich beam with a constrained damping layer subjected to axial periodic loads are studied by the finite element method. The influences of rotating speed, thickness ratio, setting angle and hub radius ratio on the resonant frequencies and modal system loss factors are presented. The regions of instability for simple and combination resonant frequencies are determined from the Mathieu equation that is obtained from the parametric excitation of the rotating sandwich beam. The regions of dynamic instability for various parameters are presented.

1. Introduction

In three-layer damped sandwich beams, the viscoelastic material (VEM) goes through considerable shear strain as the structure bends. The VEM can dissipate the energy and consequently attenuate the vibration response. In recent years, the use of viscoelastic materials as constrained damping layers to control vibration of elastic structures has been studied extensively. Kerwin [1] first discussed the damping of flexural waves due to a constrained viscoelastic layer. Di Taranto [2] derived the sixth order differential equation of motion for constrained layer damped beams with arbitrary boundary conditions. The loss factors are demonstrated to be independent of boundary conditions when a certain vibration frequency is given. Bhimaraddi [3] solved both resonant frequencies and loss factors for a simply supported sandwich beam with a constrained damping layer. In Ref. [4], Rao reformulated the problems of Ref. [2] by an energy approach and obtained exact solutions for various boundary conditions. Johnson and his co-workers [5–6] used the finite element procedure to solve the problem for beams and plates with constrained

*Corresponding author. Tel.: +886-6-275-7575x62143; fax: +886-6-235-2973.
E-mail address: chenlw@mail.ncku.edu.tw (C.-Y. Lin).

0022-460X/03/$ - see front matter
doi:10.1016/S0022-460X(02)01427-X

viscoelastic layers. Fasana and Marchesiello [7] calculated mode shapes, frequencies, and loss factors by Rayleigh–Ritz method. Polynomials which satisfy the geometric boundary conditions were chosen as admissible functions. The vibration control in machines and structures using viscoelastic damping was studied by Nakra [8]. The use of viscoelastic damping in composite laminates for the active and passive vibration control and noise suppression had been proposed by Sung and Kam [9]. The vibration control of rotating beams with an active constrained damping layer was presented by Baz and Ro [10].

The problems of the dynamic instability of beams under axial periodic loads were presented in the monograph by Bolotin [11]. The method of harmonic balance method was used to solve the Mathieu equation and obtain the unstable regions. Hsu [12] applied the perturbation and constant variation methods to a system having multiple degrees of freedom to obtain unstable regions for simple and combination resonant frequencies. Saito and Otomi [13] used Hsu's method to obtain the unstable regions for viscoelastically supported beams. Cederbaum and Mond [14] investigated the dynamic stability of a viscoelastic column subjected to a periodic longitudinal load. Kim and Kim [15] derived the governing equation from Hamilton's principle with Boltzmann's superposition principle for linear viscoelastic constitutive equation. The finite element method and the method of multiple scales were used to determine the unstability regions. The dynamic stability problems of beams and frames were also studied by Briseghella and his co-workers [16] by using the finite element method.

The dynamics of rotating beams have been an important consideration for turbomachines. Putter and Manor [17] presented the lead–lag natural frequencies of a radial beam mounted on a rotating disc at a 90° setting angle. The free vibration frequencies of rotating Timoshenko beams have been extensively studied by Yokoyama [18]. Dokainish and Rawtani [19] used a finite element technique to determine the natural frequencies and the mode shapes of a cantilever plate mounted on a rotating disc. Hoa [20] investigated the free vibration of a rotating beam with a tip mass. The setting angle was found to have a significant effect on the first mode frequencies but not on the higher frequencies. Chen and Chen [21] studied the vibration and stability of cracked thick rotating blades by the finite element method. Abbas [22] investigated the effects of rotating speed and root flexibilities on the static buckling loads and on the unstable region of a Timoshenko beam by finite element method. The dynamic stability problems of rotating blades with geometric non-linear were studied by Chen and Peng [23]. The dynamic stability of cracked rotating beams was also present by Chen and Shen [24].

In this paper, a rotating sandwich beam with a constrained damping layer subjected to an axial periodic load is studied. The effects of rotating speed, setting angle, hub radius ratio, and core thickness ratio are considered. The influences of those parameters on the resonant frequencies and modal system loss factors are discussed. The regions of instability for simple and combination resonant frequencies are determined by Hsu's method. The effects of various parameters on the dynamic stability region are also studied.

2. Finite element model

In this present study, a finite element method is applied to simulate dynamic stability problems of a rotating sandwich beam with a constrained damping layer subjected to an axial periodic load.

The geometry of a rotating sandwich beam with a fully covered viscoelastic layer is shown in Fig. 1(a). The setting angle θ is the angle between the mid-plane of the sandwich beam and the plane of rotation is shown in Fig. 1(b).

The finite element model is developed based on the following assumptions: (1) The transverse displacement w is the same for all three layers. (2) The rotary inertia and shear deformations in the constrained layer and base beam are negligible. (3) Linear theories of elasticity and viscoelasticity are used. (4) No slip occurs between the layers and there is perfect continuity at the interface. (5) Young's modulus of the viscoelastic material is negligible compared to the elastic material.

As shown in Fig. 2, the element model presented here consists of two nodes and each node has four degrees of freedom. Nodal displacements are given by

$$\{\Delta^{(e)}\} = \{u_{ci} \quad u_{bi} \quad w_i \quad \phi_i \quad u_{cj} \quad u_{bj} \quad w_j \quad \phi_j\}^{\mathrm{T}}, \tag{1}$$

where i and j are elemental node numbers. The notations u_c, u_b, w and ϕ are the axial displacement of the constrained layer, the axial displacement of the base beam, the transverse displacement and the rotational angle, respectively. They can be expressed in terms of nodal displacements and finite element shape functions.

$$u_c = [N_c]\{\Delta^{(e)}\}, \quad u_b = [N_b]\{\Delta^{(e)}\}, \quad w = [N_w]\{\Delta^{(e)}\} \quad \text{and} \quad \phi = [N_w]'\{\Delta^{(e)}\}, \tag{2}$$

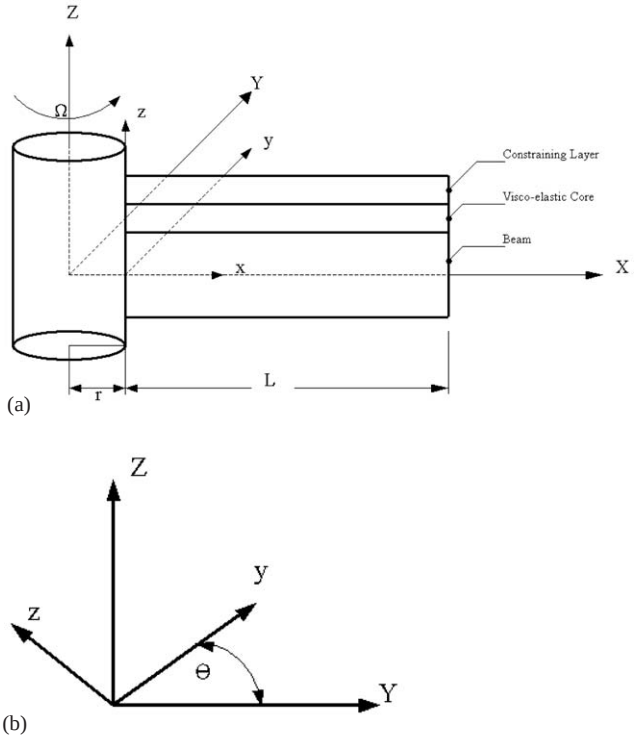

Fig. 1. The co-ordinates of the rotating sandwich beam. (a) Rotating sandwich beam with fully covered viscoelastic layer. (b) Definition of setting angle.

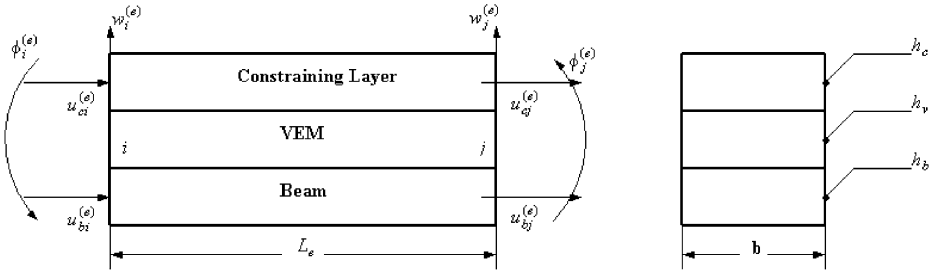

Fig. 2. A sandwich beam element.

where the prime denotes differentiation with respect to axial co-ordinate x and the shape functions are given by

$$[N_c] = [\,1-\zeta \quad 0 \quad 0 \quad 0 \quad \zeta \quad 0 \quad 0 \quad 0\,],$$

$$[N_b] = [\,0 \quad 1-\zeta \quad 0 \quad 0 \quad 0 \quad \zeta \quad 0 \quad 0\,]$$

and

$$[N_w] = [\,0 \quad 0 \quad 1-3\zeta^2+2\zeta^3 \quad (\zeta-2\zeta^2+\zeta^3)L_e \quad 0 \quad 0 \quad 3\zeta^2-2\zeta^3 \quad (-\zeta^2+\zeta^3)L_e\,], \tag{3}$$

where $\zeta = x/L_e$ and L_e is the length of the element.

2.1. Base beam and constraining layers

The potential energy of the base beam and the constrained layer is written as

$$U_k^{(e)} = \frac{1}{2}\int_0^{L_e} E_k A_k \left(\frac{\partial u_k}{\partial x}\right)^2 \mathrm{d}x + \frac{1}{2}\int_0^{L_e} E_k I_k \left(\frac{\partial w}{\partial x}\right)^2 \mathrm{d}x, \quad k = b, c, \tag{4}$$

where E, A and I are the Young's modulus, cross-section and moment of inertia, respectively. The notations b and c represent the base beam and the constraining layer, respectively.

The kinetic energy of beam and constraining layers is written as

$$T_k^{(e)} = \frac{1}{2}\int_0^{L_e} \rho_k A_k \left(\frac{\partial u_k}{\partial t}\right)^2 \mathrm{d}x + \frac{1}{2}\int_0^{L_e} \rho_k A_k \left(\frac{\partial w}{\partial t}\right)^2 \mathrm{d}x, \quad k = b, c, \tag{5}$$

where ρ is the mass density.

By substituting Eq. (2) into Eqs. (4) and (5), the element potential energy and the kinetic energy of the base beam and the constraining layer can be rewritten as

$$U_k^{(e)} = \tfrac{1}{2}\{\Delta^{(e)}\}^{\mathrm{T}}([K_{ku}^{(e)}] + [K_{kw}^{(e)}])\{\Delta^{(e)}\}, \quad k = b, c \tag{6}$$

and

$$T_k^{(e)} = \tfrac{1}{2}\{\dot{\Delta}^{(e)}\}^{\mathrm{T}}([M_{ku}^{(e)}] + [M_{kw}^{(e)}])\{\dot{\Delta}^{(e)}\}, \quad k = b, c, \tag{7}$$

where

$$[K_{ku}^{(e)}] = [K_{bu}^{(e)}] + [K_{cu}^{(e)}] = E_b A_b \int_0^{L_e} [N_b]'^{\mathrm{T}} [N_b]' \mathrm{d}x + E_c A_c \int_0^{L_e} [N_c]'^{\mathrm{T}} [N_c]' \, \mathrm{d}x,$$

$$[K_{kw}^{(e)}] = [K_{bw}^{(e)}] + [K_{cw}^{(e)}] = E_b I_b \int_0^{L_e} [N_w]''^{\mathrm{T}} [N_w]'' \, \mathrm{d}x + E_c I_c \int_0^{L_e} [N_w]''^{\mathrm{T}} [N_w]'' \, \mathrm{d}x,$$

$$[M_{ku}^{(e)}] = [M_{bu}^{(e)}] + [M_{cu}^{(e)}] = \rho_b A_b \int_0^{L_e} [N_b]^{\mathrm{T}} [N_b] \, \mathrm{d}x + \rho_c A_c \int_0^{L_e} [N_c]^{\mathrm{T}} [N_c] \, \mathrm{d}x,$$

$$[M_{kw}^{(e)}] = [M_{bw}^{(e)}] + [M_{cw}^{(e)}] = \rho_b A_b \int_0^{L_e} [N_w]^{\mathrm{T}} [N_w] \mathrm{d}x + \rho_c A_c \int_0^{L_e} [N_w]^{\mathrm{T}} [N_w] \, \mathrm{d}x$$

and the dot denotes differentiation with respect to time t.

2.2. VEM layer

The axial displacement u_v and shear strain γ_v of VEM layer derived from the kinematic relationships between the constraining layer and the base beam by Mead and Markus [25] are expressed as follows:

$$u_v = \frac{u_c + u_b}{2} + \frac{(h_c - h_b)}{4} \frac{\partial w}{\partial x} \quad \text{and} \quad \gamma_v = \frac{u_c - u_b}{h_v} + \frac{\partial w}{\partial x} \frac{(h_c + 2h_v + h_b)}{2h_v}. \tag{8}$$

By substituting Eq. (2) into Eq. (8), γ_v and u_v can be expressed in terms of nodal displacements and element shape functions:

$$u_v = [N_v]\{\Delta^{(e)}\} \quad \text{and} \quad \gamma_v = [N_\gamma]\{\Delta^{(e)}\}, \tag{9}$$

where

$$[N_v] = \frac{1}{2}([N_c] + [N_b]) + \frac{(h_c - h_b)}{4}[N_w]',$$

and

$$[N_\gamma] = \frac{([N_c] - [N_b])}{h_v} + \frac{(h_c + 2h_v + h_b)[N_w]'}{h_v}.$$

The potential energy of VEM layer due to the shear strain is written as

$$U_v^{(e)} = \frac{1}{2} \int_0^{L_e} G_v A_v \gamma_v^2 \, \mathrm{d}x, \tag{10}$$

where A_v is the cross-section area and G_v is the complex shear modulus of VEM layer.

The kinetic energy of VEM layer is written as

$$T_v^{(e)} = \frac{1}{2} \int_0^{L_e} \rho_v A_v \left\{ \left(\frac{\partial u_v}{\partial t} \right)^2 + \left(\frac{\partial w}{\partial t} \right)^2 \right\} \mathrm{d}x. \tag{11}$$

Substituting Eq. (2) into Eqs. (10) and (11), the potential energy and kinetic energy of VEM layer can be obtained

$$U_v^{(e)} = \frac{1}{2}\{\Delta^{(e)}\}^{\mathrm{T}}[K_{v\gamma}^{(e)}]\{\Delta^{(e)}\} \tag{12}$$

and

$$T_v^{(e)} = \frac{1}{2}\{\dot{\Delta}^{(e)}\}^{\mathrm{T}}[M_v^{(e)}]\{\dot{\Delta}^{(e)}\}, \tag{13}$$

where

$$[K_{v\gamma}^{(e)}] = G_v A_v \int_0^{L_e} [N_\gamma]^{\mathrm{T}}[N_\gamma]\,\mathrm{d}x$$

and

$$[M_v^{(e)}] = \rho_v A_v \int_0^{L_e} [N_v]^{\mathrm{T}}[N_v]\mathrm{d}x + \rho_v A_v \int_0^{L_e} [N_w]^{\mathrm{T}}[N_w]\mathrm{d}x.$$

2.3. Work done due to rotation

The element work of the sandwich beam due to the centrifugal forces is written as [20]

$$W_c^{(e)} = -\frac{1}{2}\int_0^{L_e} A_t\sigma_x\left(\frac{\partial w}{\partial x}\right)^2 \mathrm{d}x + \frac{1}{2}\int_0^{L_e} \rho_t A_t \Omega^2 \sin^2\theta w^2\,\mathrm{d}x, \tag{14}$$

where Ω is the rotating speed, A_t is the cross-section of the system, ρ_t is the density of the system and σ_x is the radial stress created by centrifugal forces acting on any section at a distance x from the left end of the element and can be expressed as

$$\sigma_x = \rho_t\Omega^2\left[-rx - mL_e x - \frac{x^2}{2} + c\right] \quad \text{with} \quad c = rL_e(N-m) + \frac{1}{2}L_e^2(N^2-m^2). \tag{15}$$

In the above equation, r is the hub radius, N is the total number of elements of the sandwich beam and m is the number of elements before and not including the element under consideration.

From Eq. (2) and Eq. (14), the work done by centrifugal force can be rewritten as

$$W_c^{(e)} = \tfrac{1}{2}\{\Delta^{(e)}\}^{\mathrm{T}}([K_{c1}^{(e)}] + [K_{c2}^{(e)}])\{\Delta^{(e)}\}, \tag{16}$$

where

$$[K_{c1}^{(e)}] = -\frac{1}{2}\int_0^{L_e} A_t\sigma_x[N_w]'^{\mathrm{T}}[N_w]'\,\mathrm{d}x,$$

$$[K_{c2}^{(e)}] = \rho_t A_t\Omega^2 \sin^2\theta \int_0^{L_e} [N_w]^{\mathrm{T}}[N_w]\,\mathrm{d}x.$$

2.4. Work done by axial periodic loads

The element work done by axial periodic loads $P(t)$ is written as

$$W_p^{(e)} = \frac{1}{2}\int_0^{L_e} P(t)\left(\frac{\partial w}{\partial x}\right)^2 \mathrm{d}x, \tag{17}$$

where $P(t) = P_d \cos \varpi t$, ϖ is the excitation frequency, $P_d = \beta P_{cr}$, β is the dynamic load factor and $P_{cr} = \pi^2 E_b I_b/(2L)^2$ is the critical load of the base beam.

Substituting Eq. (2) into Eq. (17), the work done by the axial periodic load can be rewritten as

$$W_p^{(e)} = \frac{1}{2}\{\Delta^{(e)}\}^{\mathrm{T}} P(t)[K_p^{(e)}]\{\Delta^{(e)}\}, \tag{18}$$

where

$$[K_p^{(e)}] = \int_0^{L_e} [N_w]'^{\mathrm{T}}[N_w]' \mathrm{d}x.$$

3. Equations of motion

The element equations of motion for a rotating sandwich beam with a constrained damping layer subjected to an axial periodic load can be derived by using the extended Hamilton's principle

$$\delta \int_{t_1}^{t_2} (T^{(e)} - U^{(e)} + W_c^{(e)} + W_p^{(e)})\, \mathrm{d}t = 0, \tag{19}$$

where $T^{(e)}$ is the element kinetic energy and $U^{(e)}$ is the element potential energy.

Substituting Eqs. (6), (7), (12), (13), (16) and (18) into Eq. (19), the element equations of motion for the sandwich beam element are obtained as follows:

$$[M^{(e)}]\{\ddot{\Delta}^{(e)}\} + [K^{(e)}]\{\Delta^{(e)}\} - \beta P_{cr} \cos \varpi t [K_P^{(e)}]\{\Delta^{(e)}\} = 0, \tag{20}$$

where

$$[M^{(e)}] = [M_{bu}^{(e)}] + [M_{bw}^{(e)}] + [M_{cu}^{(e)}] + [M_{cw}^{(e)}] + [M_v^{(e)}]$$

and

$$[K^{(e)}] = [K_{bu}^{(e)}] + [K_{bw}^{(e)}] + [K_{cu}^{(e)}] + [K_{cw}^{(e)}] + [K_{v\gamma}^{(e)}] + [K_{c1}^{(e)}] - [K_{c2}^{(e)}].$$

Assembling of each element, the equations of motion of global system can be expressed as

$$[M]\{\ddot{\Delta}\} + [K]\{\Delta\} - \beta P_{cr} \cos \varpi t [K_p]\{\Delta\} = 0. \tag{21}$$

In order to obtain an approximate solution, the nodal displacements $\{\Delta\}$ can be assumed as

$$\{\Delta\} = [\Phi]\{\Gamma\}, \tag{22}$$

where $[\Phi]$ is a normalized modal matrix of $[M]^{-1}[K]$ and $\{\Gamma\}$ is a new set of generalized coordinates. Substitute Eq. (22) into Eq. (21), the Eq. (21) can be transformed to the following N coupled Mathieu equations:

$$\ddot{\Gamma}_m + (\omega_m^*)^2 \Gamma_m + \beta P_{cr} \cos(\varpi t) \sum_{n=1}^{N} b_{mn}^* \Gamma_n = 0, \quad m = 1, 2, \ldots, N, \tag{23}$$

where $(\omega_m^*)^2$ are the eigenvalues of $[M]^{-1}[K]$ and b_{mn}^* are the elements of the complex matrix $[B] = -[\Phi]^{-1}[M]^{-1}[K_p][\Phi]$. ω_m^* and b_{mn}^* are written as

$$\omega_m^* = \omega_{m,R} + \mathrm{i}\omega_{m,I}, \quad b_{mn}^* = b_{mn,R} + ib_{mn,I} \quad \text{and} \quad \mathrm{i} = \sqrt{-1}.$$

4. Regions of instability

The boundaries of unstable regions are studied in this section. Hsu's [12] procedure is applied to solve the Mathieu Eq. (23) and the regions of instability for simple and combination resonances of sum and difference types have been determined. The results are obtained as follows.

(A) *Simple resonance:* In this case, the boundaries of the unstable regions are given by

$$\left|\frac{\varpi}{2\omega_0} - \bar{\omega}_{\mu,R}\right| < \frac{1}{4}\left[\frac{\beta^2(b_{\mu\mu,R}^2 + b_{\mu\mu,I}^2)}{\bar{\omega}_{\mu,R}^2} - 16\bar{\omega}_{\mu,I}^2\right]^{1/2}, \mu = 1, 2, \ldots, N, \tag{24}$$

where

$$\omega_0 = \sqrt{E_b I_b/\rho_b A_b L^4}, \quad \bar{\omega}_{\mu,R} = \omega_{\mu,R}/\omega_0 \quad \text{and} \quad \bar{\omega}_{\mu,I} = \omega_{\mu,I}/\omega_0.$$

When damping is negligible, the unstable regions are

$$\left|\frac{\varpi}{2\omega_0} - \bar{\omega}_{\mu,R}\right| < \frac{1|\beta b_{\mu\mu,R}|}{4\ \bar{\omega}_{\mu,R}}, \mu = 1, 2, \ldots, N. \tag{25}$$

(B) *Combination resonance of sum type:* The boundaries of the unstable regions in this case are given by

$$\left|\frac{\varpi}{2\omega_0} - \frac{1}{2}(\bar{\omega}_{\mu,R} + \bar{\omega}_{\nu,R})\right| < \frac{(\bar{\omega}_{\mu,I} + \bar{\omega}_{\nu,I})}{8(\bar{\omega}_{\mu,I}\bar{\omega}_{\nu,I})^{1/2}}\left[\frac{\beta^2(b_{\mu\nu,R}b_{\nu\mu,R} + b_{\mu\nu,I}b_{\nu\mu,I})}{\bar{\omega}_{\mu,R}\bar{\omega}_{\nu,R}} - 16\bar{\omega}_{\mu,I}\bar{\omega}_{\nu,I}\right]^{1/2},$$
$$\mu \neq \nu, \quad \mu, \nu = 1, 2, \ldots, N. \tag{26}$$

When damping is negligible, the unstable regions are

$$\left|\frac{\varpi}{2\omega_0} - \frac{1}{2}(\bar{\omega}_{\mu,R} + \bar{\omega}_{\nu,R})\right| < \frac{1}{4}\left[\frac{\beta^2(b_{\mu\nu,R}b_{\nu\mu,R})}{\bar{\omega}_{\mu,R}\bar{\omega}_{\nu,R}}\right]^{1/2},$$
$$\mu \neq \nu, \quad \mu, \nu = 1, 2, \ldots, N. \tag{27}$$

(C) *Combination resonance of difference type:* The boundaries of the unstable regions in this case are given by

$$\left|\frac{\varpi}{2\omega_0} - \frac{1}{2}(\bar{\omega}_{\nu,R} - \bar{\omega}_{\mu,R})\right| < \frac{(\bar{\omega}_{\mu,I} + \bar{\omega}_{\nu,I})}{8(\bar{\omega}_{\mu,I}\bar{\omega}_{\nu,I})^{1/2}}\left[\frac{\beta^2(b_{\mu\nu,I}b_{\nu\mu,I} - b_{\mu\nu,R}b_{\nu\mu,R})}{\bar{\omega}_{\mu,R}\bar{\omega}_{\nu,R}} - 16\bar{\omega}_{\mu,I}\bar{\omega}_{\nu,I}\right]^{1/2},$$
$$\nu > \mu, \mu, \quad \nu = 1, 2, \ldots, N. \tag{28}$$

When damping is negligible, the unstable regions are

$$\left|\frac{\varpi}{2\omega_0}-\frac{1}{2}(\bar{\omega}_{\mu,R}+\bar{\omega}_{v,R})\right|<\frac{1}{4}\left[\frac{\beta^2(-b_{\mu v,R}b_{v\mu,R})}{\bar{\omega}_{\mu,R}\bar{\omega}_{v,R}}\right]^{1/2},\ v>\mu,\quad \mu,v=1,2,\ldots,N. \tag{29}$$

5. Numerical results and discussion

The vibration and dynamic stability problems of the rotating sandwich beam with a constrained damping layer are studied by the finite element method. The effects of rotating speed, core thickness ratio, setting angle and hub radius ratio are considered.

The resonant frequencies and modal loss factors of the cantilever sandwich beam with various values of loss factor of VEM are solved in Table 1 and compared with the results of Ref. [4]. The resonant frequencies of rotating beams with different rotating speeds are also obtained in Table 2 and the results compared with Ref. [17]. We can see that the present results are in good agreement with those of Refs. [4] and [17].

The dynamic behaviors of the rotating sandwich beam with a constrained damping layer are first investigated. The materials properties and geometrical parameters are shown in Table 3. Let $P(t)=0$, the characteristic eigenvalue equations of a rotating sandwich beam can be obtained from the resulting equations:

$$\{[K]-(\omega^*)^2[M]\}\{\Phi\}=0, \tag{30}$$

where ω^* is complex radian frequency (rad/s) and $\{\Phi\}$ is corresponding eigenvector. The complex eigenvalues $(\omega^*)^2$ is expressed

$$(\omega^*)^2=\omega^2(1+\mathrm{i}\eta), \tag{31}$$

where η is the modal system loss factor and ω is the resonant frequency.

The effects of rotating speed (Ω), core thickness ratio (h_v/h_b), setting angle (θ) and hub radius ratio (r/L) on the resonant frequencies and modal loss factors are shown in Figs. 3–6, respectively. The effect of the rotating speed is presented in Fig. 3. It can be seen that the resonant frequency increases and modal system loss factor decreases with the increasing of the rotating speed. The

Table 1
Comparison of results of the cantilever VEM sandwich beam, f(Hz)-resonant frequency, $\bar{\eta}$-modal loss factors (=modal system loss factor/core loss factor)

η_c		f_1	$\bar{\eta}_1$	f_2	$\bar{\eta}_2$	f_3	$\bar{\eta}_3$	f_4	$\bar{\eta}_4$
0.1	Ref. [4]	64.1	0.2815	296.4	0.2424	743.7	0.1540	1393.9	0.0889
	Present	63.8	0.2850	295.4	0.2483	745.0	0.1584	1404.5	0.0915
0.6	Ref. [4]	65.5	0.2460	298.9	0.2323	745.5	0.1528	1394.9	0.0886
	Present	65.4	0.2492	298.5	0.2384	747.3	0.1572	1405.5	0.0913
1	Ref. [4]	67.4	0.2022	302.8	0.2177	748.6	0.1502	1396.6	0.0881
	Present	67.5	0.2053	303.3	0.2241	751.4	0.1550	1407.4	0.0910
1.5	Ref. [4]	69.9	0.1531	308.9	0.1975	754.0	0.1460	1399.7	0.0873
	Present	70.1	0.1559	310.7	0.2044	759.0	0.1513	1410.9	0.0905

Table 2
Comparisons of results of a rotating beam for first two resonant frequencies ($\omega\sqrt{\rho AL^4/EI}$), where $\Omega' = \Omega\sqrt{\rho AL^4/EI}$, $R = r/L$, $\theta = 90^\circ$

Ω'		Mode 1		Mode 2	
		$R = 0$	$R = 1$	$R = 0$	$R = 1$
2	Present work	3.623	4.403	22.528	23.282
	Ref [17]	3.612	4.401	22.526	23.280
5	Present work	4.075	7.415	24.952	28.927
	Ref. [17]	4.074	7.412	24.95	28.924
10	Present work	5.052	13.261	32.124	43.238
	Ref. [17]	5.049	13.258	32.12	43.227

Table 3
Material properties and geometrical parameters

Young's modulus E_b, E_c (GPa)	70
Shear modulus G (MPa)	0.2615
Base beam thickness h_b (m)	0.0015
Constrained layer thickness h_c (m)	0.00015
Loss factor of VEM η_c	0.38
Length (m)	0.3 m
Density ρ_b, ρ_c (kg/m^3)	2800
Density ρ_v (kg/m^3)	1100

effect of the core thickness ratio is illustrated in Fig. 4. It shows that the resonant frequencies decrease with an increase in core thickness ratio. The modal system loss factor increases as the core thickness ratio increases. In Fig. 5, the influence of setting angle is discussed. The resonant frequencies decrease and the modal system loss factor increase as the setting angle increases. But, it is observed that the changes of the second mode for the resonant frequency and modal system loss factor due to θ are very small. Since $\Omega^2 \sin^2\theta$ does not change with different modes, the effect of setting angle becomes negligible beyond the second mode. The effects of hub radius ratio are studied in Fig. 6. The resonant frequency increases as the hub radius increases. The modal system loss factor decreases rapidly as the hub radius ratio increases.

The dynamic instability of a rotating sandwich beam with a constrained damping layer subjected to an axial periodic load is studied in the following discussions. The effects of rotating speed, setting angle, hub radius ratio and core thickness ratio for the stability boundaries are presented in Figs. 7–14, respectively. The effects of the rotating speed on the dynamic stability of the rotating sandwich beam are shown in Figs. 7–8. Fig. 7 illustrates that increasing of the rotating speed will increase the excitation frequency (ϖ) so that the unstable regions shift to the right. The width of unstable region (w_{ur}) decreases and the critical excitation parameter (β_{cr}) increases when rotating speed increases that shown in Fig. 8. The critical excitation parameter can be determined as the radical in Eqs. (24), (26) and (28) is equal to zero and the width of unstable

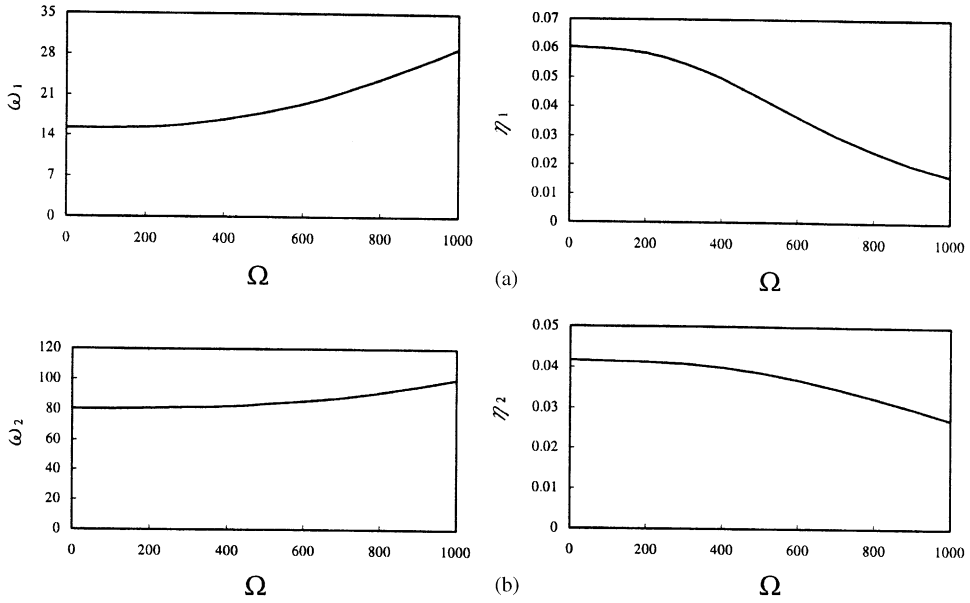

Fig. 3. The effect of rotating speed Ω (r.p.m.) on resonant frequencies ω (Hz) and modal system loss factors η, where $r/L = 0$, $h_v/h_b = 0.5$, and $\theta = 0^\circ$; (a) first mode, (b) second mode.

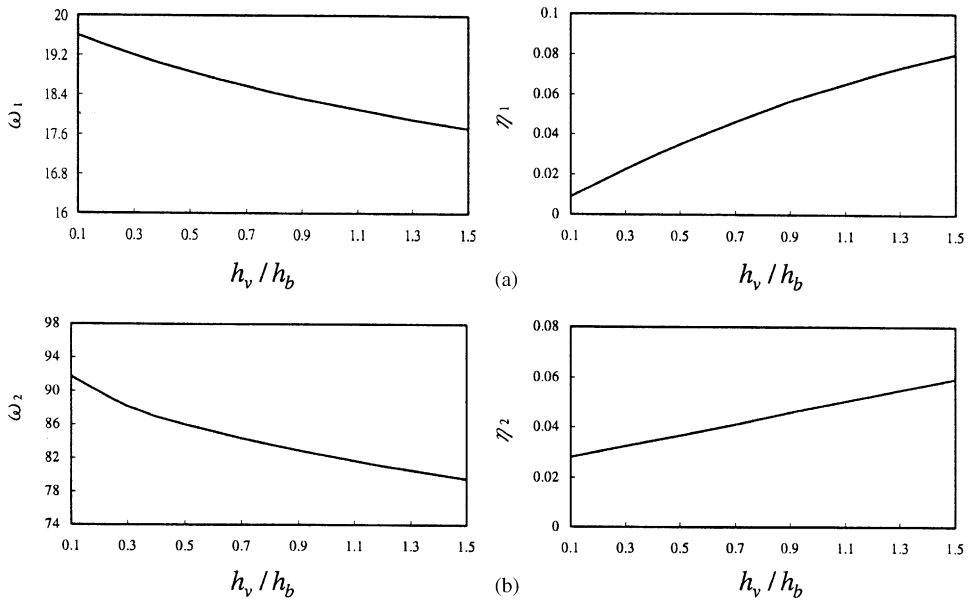

Fig. 4. The effect of thickness ratio h_v/h_b on resonant frequencies ω (Hz) and modal system loss factors η, where $\Omega = 1000$ (r.p.m.), $r/L = 0$, and $\theta = 0^\circ$; (a) first mode, (b) second mode.

region is calculated at $\beta = 0.5$. Obviously, the higher rotating speed will increase the stiffness of the sandwich beam and make the sandwich beam more stable. Figs. 9 and 10 illustrate the effects of the setting angle on the dynamic stability of a rotating sandwich beam. We can see that the

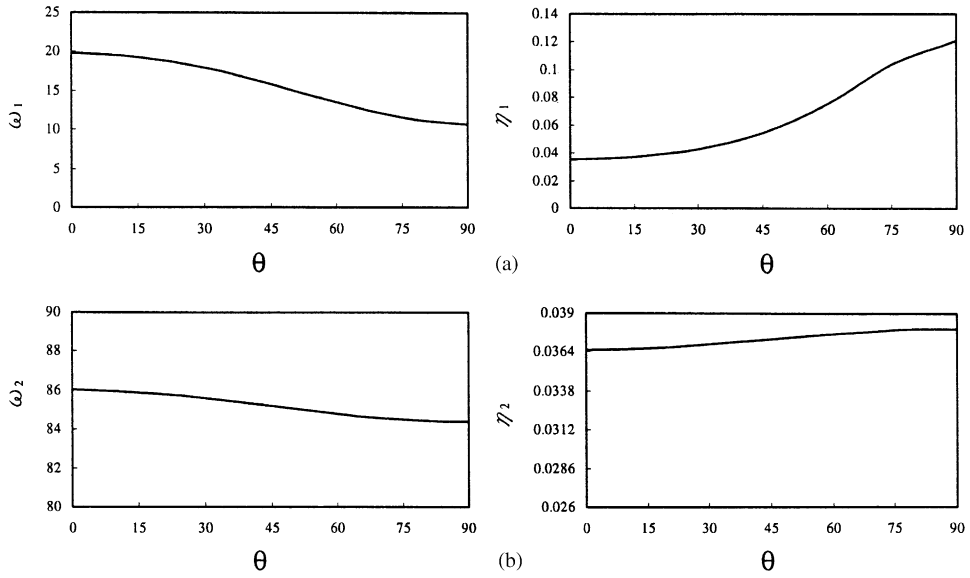

Fig. 5. The effect of setting angle θ (degrees) on resonant frequencies ω (Hz) and modal system loss factors η, where $\Omega = 1000$ (r.p.m.), $h_v = 0.5h_b$, and $r/L = 0$; (a) first mode, (b) second mode.

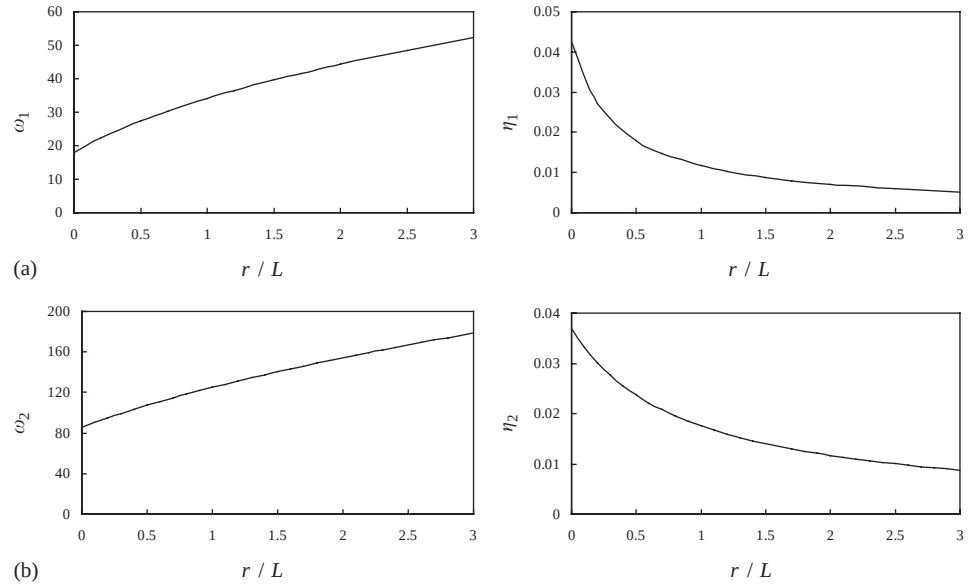

Fig. 6. The effect of hub radius ratio (r/L) on resonant frequencies ω (Hz) and modal system loss factors η, where $\Omega = 1000$ (r.p.m.), $h_v = 0.5h_b$, and $\theta = 30^\circ$; (a) first mode, (b) second mode.

unstable regions shift to left when the setting angle increases. It is due to the decrease of the resonant frequency. But, the simple resonance ω_2 is changed very slightly so that the effect of setting angle on the dynamic stability problem is negligible for higher simple resonances. Fig. 10 shows that the width of unstable regions increases as the setting angle increases and the critical

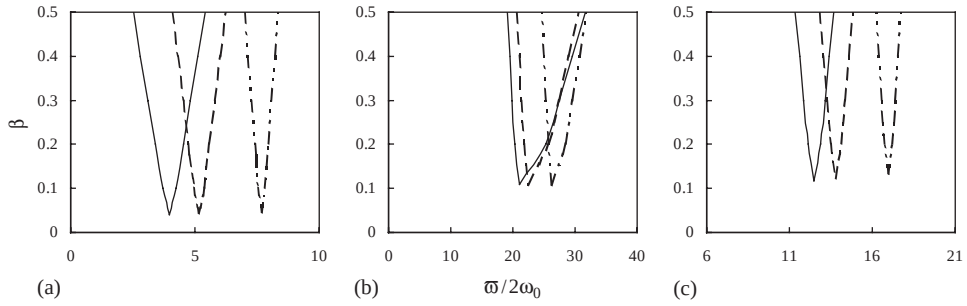

Fig. 7. Stability boundaries for various rotating speeds Ω: $\theta = 0$, $r/L = 0$, and $h_v/h_b = 0.5$; (a) ω_1, (b) ω_2, (c) $\omega_1 + \omega_2$; —— $\Omega = 0$; – – – – $\Omega = 1000$ r.p.m.; –·· ·–·· ·– $\Omega = 2000$ r.p.m.

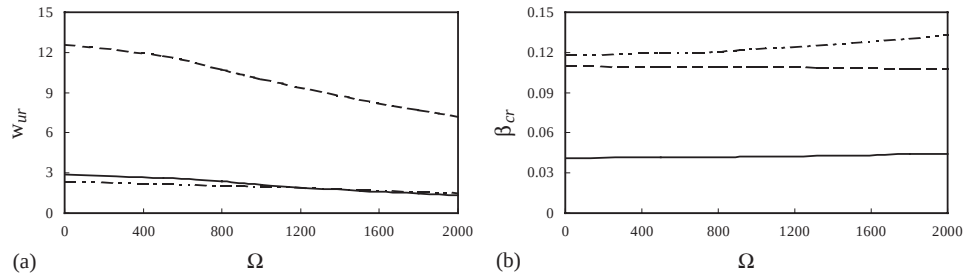

Fig. 8. The effects of rotating speed Ω on the width of unstable region (w_{ur}) and critical excitation parameter (β_{cr}): $\theta = 0^\circ$, $r/L = 0$, $h_v/h_b = 0.5$ and $\beta = 0.5$; —— ω_1; – – – – ω_2; –· ·– $\omega_1 + \omega_2$.

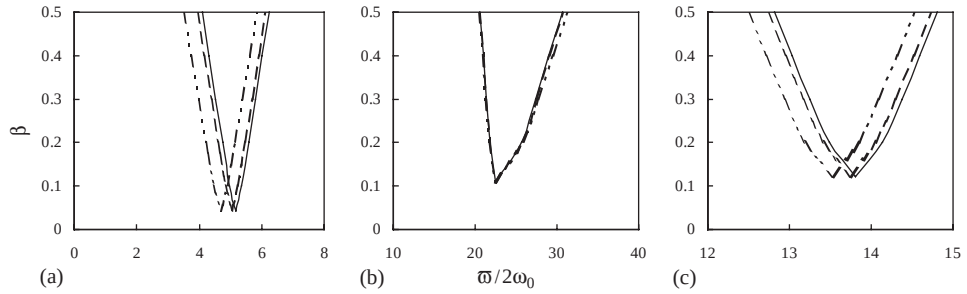

Fig. 9. Stability boundaries for various setting angles θ: $\Omega = 1000$ r.p.m., $r/L = 0$, and $h_v/h_b = 0.5$; (a) ω_1, (b) ω_2, (c) $\omega_1 + \omega_2$; —— $\theta = 0^\circ$; – – – – $\theta = 15^\circ$; –· ·– $\theta = 30^\circ$.

excitation parameter changes slightly due to the increase of setting angles. It shows that the rotating beam with a larger setting angle will get lower system stiffness. Consequently, increasing the setting angle makes the rotating sandwich beam more unstable. The effects of the hub radius ratio on the dynamic stability of the rotating sandwich beam are shown in Figs. 11–12. Fig. 11 shows that the unstable regions shift to the right as the hub radius ratio increases. The width of unstable region decreases as hub radius ratio increases shown in Fig. 12(a). The critical excitation parameter changes slightly as the hub radius ratio increases as shown in Fig. 12(b). This case shows that larger hub radius ratio makes the rotating sandwich beam more stable. Figs. 13 and 14

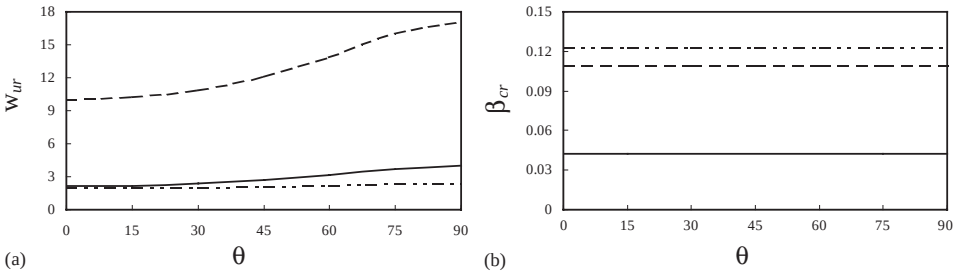

Fig. 10. The effects of setting angle θ on the width of unstable region (w_{ur}) and critical excitation parameter (β_{cr}): $\Omega = 1000$ r.p.m., $r/L = 0$, $h_v/h_b = 0.5$ and $\beta = 0.5$;—— ω_1; – – – – ω_2; –·–·–·– $\omega_1 + \omega_2$.

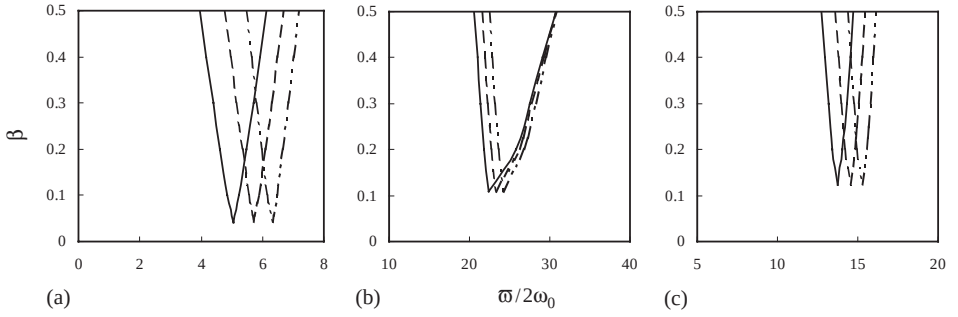

Fig. 11. Stability boundaries for various hub radius ratios r/L: $\Omega = 1000$ r.p.m., $\theta = 30^\circ$, and $h_v/h_b = 0.5$; (a) ω_1, (b) ω_2, (c) $\omega_1 + \omega_2$; —— $r/L = 0$;– – – – $r/L = 0.5$; –·–·–·– $r/L = 1$.

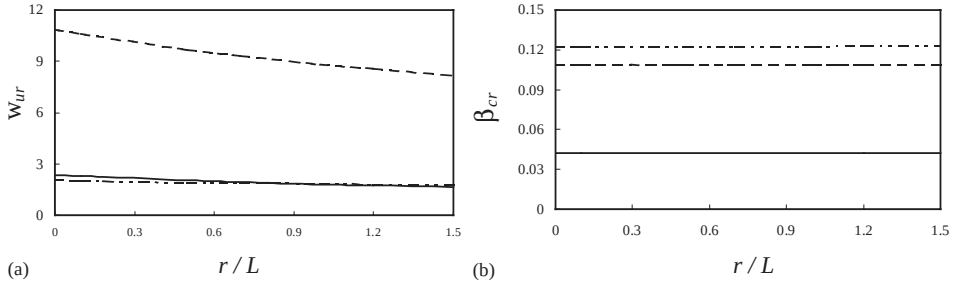

Fig. 12. The effects of hub radius ratio r/L on the width of unstable region (w_{ur}) and critical excitation parameter (β_{cr}): $\Omega = 1000$ r.p.m., $\theta = 30^\circ$, $h_v/h_b = 0.5$ and $\beta = 0.5$; —— ω_1; – – – – ω_2; –·–·–·– $\omega_1 + \omega_2$.

illustrate the effects of the core thickness ratio on the dynamic stability of the rotating sandwich beam. The unstable regions for different core thickness ratio are shown in Fig. 13. As the core thickness ratio increases, the excitation frequency decreases so that the unstable region shifts to the left. The higher core thickness ratio induces higher damping effect so that the values of the critical excitation parameter increase due to the increase of the core thickness ratio. The width of unstable region decreases with an increase in the core thickness ratio. Consequently, the larger thickness ratio makes the rotating sandwich beam more stable.

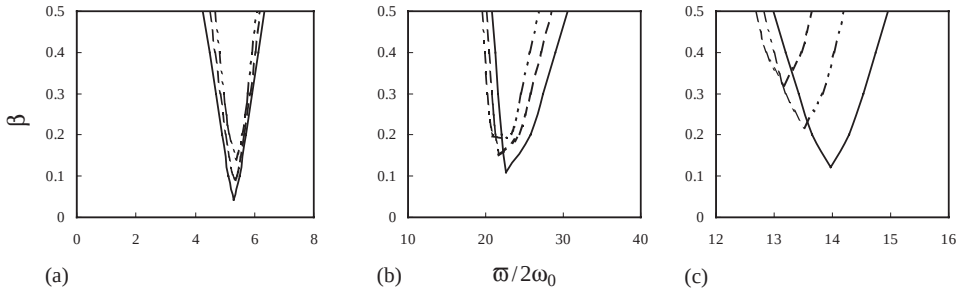

Fig. 13. Stability boundaries for various thickness ratios h_v/h_b: $\Omega = 1000$ r.p.m., $\theta = 0^\circ$, and $r/L = 0.1$; (a) ω_1, (b) ω_2, (c) $\omega_1 + \omega_2$; —— $h_v/h_b = 0.5$; – – – – $h_v/h_b = 1$; –·· ··–·· ··– $h_v/h_b = 1.5$.

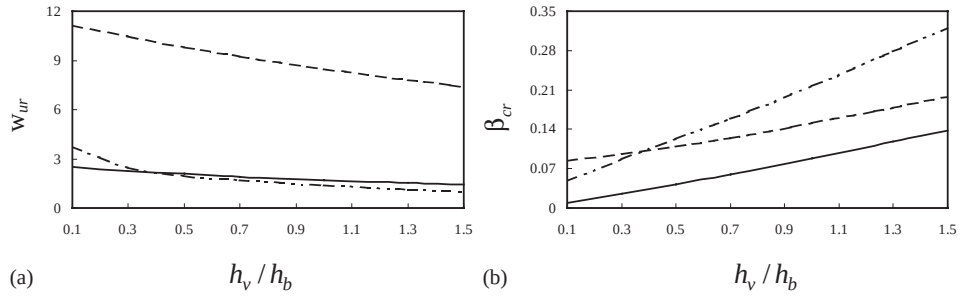

Fig. 14. The effects of thickness ratio h_v/h_b on the width of unstable region (w_{ur}) and critical excitation parameter (β_{cr}): $\Omega = 1000$ r.p.m., $\theta = 0^\circ$, $r/L = 0.1$ and $\beta = 0.5$; —— ω_1; – – – – ω_2; –·· ··–·· ··– $\omega_1 + \omega_2$.

6. Conclusion

The dynamic stability of a rotating sandwich beam with a constrained damping layer has been studied by the finite element method. The effects of rotating speed, setting angle, hub radius ratio and core thickness ratio have been examined. Increasing the rotating speed, hub radius and thickness of VEM layer will decrease the width of unstable region and increase the critical excitation parameter of the sandwich beam. The system is more stable as the rotating speed, hub radius and thickness of VEM layer increase. The larger setting angle will reduce the stiffness of the rotating sandwich beam. The rotating sandwich beam is more unstable at the large setting angle. It is noted that the effect of the setting angle on the dynamic stability problem can be negligible for higher simple resonant frequency case.

Appendix A. Nomenclature

$A_{b,c,v}$	cross-section of base beam, constrained layer and VEM layer
A_t	cross-section of system
b	beam width
$E_{b,c}$	Young's modulus of base beam and constrained layer
G	shear modulus of VEM

G_v	complex shear modulus of VEM $G_v = G(1 + i\eta_c)$
$h_{b,c,v}$	thickness of base beam, constrained layer and VEM layer
$I_{b,c}$	moment of inertia of base beam and constrained layer
$[K]$	global stiffness matrix
L_e	length of a element
L	beam length
m	number of elements before and not including the element under consideration
$[M]$	global mass matrix
N	total number of elements
$N_{c,b,w,v,\gamma}$	shape function of the axial displacement of the constrained layer, the axial displacement of the base beam, the transverse displacement, the axial displacement of VEM layer and the shear strain of VEM layer
P_d	dynamic and static load
P_{cr}	critical load of base beam $P_{cr} = \pi^2 E_b I_b/(2L)^2$
r	hub radius
$u_{b,c}$	axial deformation of base beam and constrained layer
w	transverse displacement
w_{ur}	width of unstable region
Ω	rotating speed
θ	setting angle
γ_v	shear strain of VEM layer
$\rho_{b,c,v}$	mass density of base beam, constrained layer and VEM layer
ρ_t	mass density of system
$\{\Delta\}$	nodal displacement vector
η	modal system loss factor
η_c	loss factor of VEM layer
$\bar{\eta}$	modal system loss factor/loss factor of VEM layer, $\bar{\eta} = \eta/\eta_c$
ω^*	complex radian frequency
ϖ	excitation radian frequency
ω	resonant frequency
ω_0	frequency of base beam, $\omega_0 = \sqrt{E_b I_b/\rho_b A_b L^4}$
$\bar{\omega}$	non-dimensional frequency, $\bar{\omega} = \omega/\omega_0$
β	dynamic load factor
β_{cr}	critical excitation parameter
$\{\Phi\}$	corresponding eigenvector of $[M]^{-1}[K]$
ϕ	rotational angle

References

[1] E.M. Kerwin, Damping of flexural waves by a constrained viscoelastic layer, Journal of the Acoustical Society of America 31 (7) (1959) 952–962.

[2] R.A. Ditaranto, Theory of vibratory bending of elastic and viscoelastic layered finite-length-beams, Journal of Applied Mechanics Transactions of the American Society Series E 87 (1965) 881–887.

[3] A. Bhimaraddi, Sandwich beam theory and the analysis of constrained layer damping, Journal of Sound and Vibration 179 (1995) 591–602.
[4] D.K. Rao, Frequency and loss factors of sandwich beams under various boundary conditions, Journal of Mechanical Engineering Science 20 (1978) 271–282.
[5] C.D. Johnson, D.A. Kienholz, L.C. Rogers, Finite element prediction of damping in beams with constrained viscoelastic layers, Shock and Vibration Bulletin 51 (1) (1981) 71–81.
[6] C.D. Johnson, D.A. Kienholz, Finite element prediction of damping in structures with constrained viscoelastic layers, American Institute of Aeronautics and Astronautics Journal 20 (9) (1981) 1284–1290.
[7] A. Fasana, S. Marchesiello, Rayleigh-Ritz analysis of sandwich beams, Journal of Sound and Vibration 241 (4) (2001) 643–652.
[8] B.C. Nakra, Vibration control in machines and structures using viscoelastic damping, Journal of Sound and Vibration 211 (3) (1998) 449–465.
[9] Y. Sung, Y.S. Kam, A finite element formulation for composite laminates with smart constrained layer damping, Advances in Engineering Software 31 (2000) 529–537.
[10] A. Baz, J. Ro, Vibration control of rotating beams with active constrained layer damping, Smart Materials and Structures 10 (2001) 112–120.
[11] Bolotin, the Dynamic Instability of Elastic Systems, Holden-Day, London, 1964.
[12] C.S. Hsu, On the parametric excitation of a dynamic system having multiple degrees of freedom, Journal of Applied Mechanics, Transactions of the American Society of Mechanical Engineers 30 (1963) 367–372.
[13] H. Saito, K. Otomi, Parametric response of viscoelastically supported beams, Journal of Sound and Vibration 63 (2) (1979) 169–178.
[14] G. Cederbaum, M. Mond, Stability properties of a viscoelastic column under a periodic force, Journal of Applied Mechanics, Transactions of the American Society of Mechanical Engineers 59 (1992) 16–19.
[15] T.W. Kim, J.H. Kim, Parametric instability of a cross-ply laminated beam with viscoelastic properties under a periodic force, Composite Structures 51 (2001) 205–209.
[16] L. Briseghella, C.E. Majorana, C. Pellegrino, Dynamic stability of elastic structures: a finite element approach, Computers and Structures 69 (1998) 11–25.
[17] S. Putter, H. Manor, Natural frequencies of radial rotating beams, Journal of Sound and Vibration 56 (2) (1978) 175–185.
[18] T. Yokoyama, Free vibration characteristics of rotating Timoshenko beam, International Journal of Mechanical Sciences 30 (10) (1988) 743–755.
[19] M.A. Dokainish, S. Rawtani, Vibration analysis of rotating cantilever plates, International Journal for Numerical Methods in Engineering 3 (1971) 233–248.
[20] S.V. Hoa, Vibration of a rotating beam with tip mass, Journal of Sound and Vibration 67 (3) (1979) 369–381.
[21] L.W. Chen, C.L. Chen, Vibration and stability of cracked thick rotating blades, Computers and Structures 28 (1) (1988) 67–74.
[22] B.A.H. Abbas, Dynamic stability of a rotating Timoshenko beam with a flexible root, Journal of Sound and Vibration 108 (1) (1986) 25–32.
[23] L.W. Chen, W.K. Peng, Dynamic stability of rotating blades with geometric non-linearity, Journal of Sound and Vibration 187 (3) (1995) 421–433.
[24] L.W. Chen, G.S. Shen, Dynamic stability of cracked rotating beams of general orthotropy, Composite Structures 37 (1997) 165–172.
[25] D.J. Mead, S. Markus, The forced vibration of a three-layer damped sandwich beam with arbitrary boundary conditions, Journal of Sound and Vibration 10 (1969) 163–175.